

Hydrogenolysis of Glycerol by Heterogeneous Catalysis: A Fractional Order Kinetic Model with Analysis

Changjin Xu^{a*}, Maoxin Liao^b, Muhammad Farman^{c,d,e},
Aamir Shehzad^e

^a *Guizhou Key Laboratory of Economics System Simulation, Guizhou
University of Finance and Economics, Guiyang 550025, PR China*

^b *School of Mathematics and Physics, University of South China,
Hengyang 421001, PR China*

^c *Mathematics Research Center, Department of Mathematics, Near East
University, 99138 Nicosia, Cyprus, Turkey*

^d *Department of Computer Science and Mathematics, Lebanese American
University, 1102-2801, Beirut, Lebanon*

^e *Institute of Mathematics, Khawaja Fareed University of Engineering
and Information Technology, Rahim Yar Khan 64200, Pakistan*

xcj403@126.com, maoxinliao@126.com, farmanlink@gmail.com,

aamir.shehzad.1054@gmail.com

(Received October 13, 2023)

Abstract

The demand for glycerol, a by-product of biodiesel manufacturing, is anticipated to surpass supply, necessitating efficient conversion techniques for sustainability. The importance of effective conversion techniques is illustrated by the development of a system of fractional order differential equations using a literature reaction model. This study focuses on understanding and describing potential glycerol hydrogenolysis pathways by investigating the kinetics of

*Corresponding author.

a catalyzed hydrogenolysis model using qualitative analysis of fractional order differential equations, as there is limited research on the underlying reactions. The model is analyzed qualitatively and quantitatively using fixed point theorems. It is found to be generalized Ulam-Hyers-Rassias stable. The impact of the fractional operator is studied through computational simulations using a two-step Lagrange polynomial. Graphs at different fractional derivative orders show the significant influence of the fractional order on the model's classes. Even though the results are based on a particular kinetic model, they aim to improve comprehension and description of the process.

1 Introduction

Human activities like climate change, air pollution, and urbanization negatively impact the environment, leading to higher temperatures and changing precipitation patterns, prompting researchers to seek solutions [1]. Prior to civilization, the end of the Ice Age and the Industrial Revolution both dramatically raised greenhouse gas concentrations [2]. The environmental effects of the industrial age can be seen in the rise in atmospheric carbon dioxide content during the previous 0.8 million years [3]. Pollution is a result of using fossil fuels, especially when producing food, transporting individuals around, and destroying forests. Waste decomposition also increases greenhouse gas emissions, demonstrating the urgency of combating climate change [4]. Climate change and problems with fossil fuels are related to the threats to the environment posed by dangerous carbon dioxide emissions and particulate matter [5]. Due to their affordability and versatility, biodiesel and bio-compressed natural gas are eco-friendly, non-toxic alternatives. In place of petroleum diesel in transportation, biodiesel, a blend of fatty acids and alkyl esters, is biodegradable, renewable, and environmentally friendly. It is a well-liked option in the manufacturing industries because of its higher lubricity, which increases engine efficiency and longevity [6]. Biodiesel manufacturing is crucial for efficiency and affordability, with large volumes of glycerol produced as a by-product. Increased production has made glycerol abundant, making it a desirable platform chemical [7].

Glycerol is a naturally occurring, non-toxic liquid that is utilized in a

number of sectors, including the chemical, food, and pharmaceutical industries [8]. Crude glycerol, a byproduct of biodiesel, is normally removed using centrifugation or gravity separation. This crude glycerol could be contaminated with salt, oil, soap, methanol, and other organic substances. Effective use of crude glycerol is essential to making biodiesel more economically sustainable and reducing its environmental impact. Its utility and worth can be increased by lowering these pollutants [9]. 3.28 million tonnes of glycerol were created as a byproduct of the 32.8 million tonnes of biodiesel that were produced globally in 2016. This is essential for the long-term viability and affordability of the manufacturing of biodiesel [10]. Glycerol is produced in excess as output rises, and it can be converted into a variety of compounds through the use of catalysts and processes [11]. Since 2000, over 1000 publications have explored catalytic hydrogenolysis of glycerol to useful compounds, breaking chemical bonds and adding hydrogen to glycerol, a saturated molecule with higher O/C content [12,13]. With the aid of a metal catalyst, hydrogenolysis disassembles the chemical bonds in glycerol to provide ethanol, propanol, methane, and primary products such 1,2-propanediol, 1,3-propanediol, and ethylene glycol. Ink, fiber glass, cosmetics, and coolants are just a few of the industrial operations that utilize these products [14]. Numerous researchers have conducted in-depth study on the development of selective hydrogenolysis of glycerol employing a variety of catalysts [15–17].

Research on the hydrogenolysis of glycerol using catalysts makes considerable use of mathematical modeling [18–20]. Fractional-order, involving integration and transect differentiation, aids in understanding real-world problems and modeling phenomena due to memory and hereditary properties [21–23]. Component concentration is important for chemical and nonlinear problems in kinetics chemistry and is improved by fractional-order modeling, which incorporates integration and transect differentiation [24]. Using fractional time derivatives and the q-homotopy analysis transform method, Saad K.M. [25] created a novel model for a cubic isothermal auto-catalytic chemical system and offered approximations of the solutions. Researchers [26] studied the distinctness of the fractional-order delayed Brusselator chemical reaction model using contraction map-

ping, providing a suitable condition to guarantee stability and the beginning of Hopf bifurcation. Another study [27] used the Atangana-Baleanu time-fractional operator and the Mittag-Leffler kernel to transform the nonlinear differential equations into fractional-order models in order to investigate the substrate-enzyme reversible reaction. The Newton polynomial interpolation technique-based Atangana-Toufik approach was utilized to provide numerical results. Recent studies have shown control strategies, hopf bifurcation, and stability in fractional order systems [28, 29]. Numerous investigations were also carried out by researchers to improve the ecological systems and the environment [30, 31].

In this study, we concentrate on the reaction mechanisms for potential glycerol hydrogenolysis pathways. Since there is little research on the underlying reactions, the goal of this work is to improve the tools for better understanding and describing the reaction by investigating the kinetics of a catalyzed hydrogenolysis model utilizing qualitative analysis of fractional order differential equations. A generalized version of the model and a summary of the description of the proposed model are provided in Section “2”. Furthermore, the theoretical background of the suggested fractional operator is explored. Section 3” deals with the qualitative analysis of the proposed system. The numerical solutions to the suggested fractional-order model with power law kernel are provided in Section “4”. In Sections “5” and “6,” the numerical simulations, results, and conclusions will be addressed.

2 Kinetic model for glycerol hydrogenolysis via heterogeneous catalysis

The hydrogenolysis of glycerol involves cleaving glycerol’s chemical bonds with hydrogen in the presence of a metal catalyst, producing main products like 1,2-propanediol (1,2-PD), 1,3-propanediol (1,3-PD), and ethylene glycol (EG), as well as secondary products like ethanol, propanol, and methane. For the sake of this investigation, we take into account one reaction from [20]. The Cu-Re/ZnO catalyst is used in this reaction. The

concentration of the catalyst and the hydrogen pressure are non-zero constants in order to study the kinetic model. The quantity of every substance other than glycerol and hydrogen is zero at the beginning time $t = 0$. We use the symbols \mathbf{X}_1 for glycerol and \mathbf{X}_2 for glyceraldehyde to represent them. We also begin with the presumption that the concentrations of glycolaldehyde and formic acid are equal at the beginning of the process, ensuring that their amounts at any subsequent time will also be equal and will be indicated by \mathbf{X}_3 . The symbol \mathbf{X}_4 designates the primary product, ethylene glycol. We do not differentiate between 1,2-propanediol(1,2-PD) and 1,3-propanediol(1,3-PD) because, as was briefly discussed in [20], the latter is said to have been generated in extremely small quantities. Instead, we use the symbol \mathbf{X}_5 to indicate their global concentration. The corresponding parameter values can be determined using experimental data from the prior studies, as mentioned in [20]. Fractional calculus is crucial for understanding complex physical systems dynamics, as its non-local nature allows for accurate representation of natural phenomena and control of various mathematical models. Therefore, we use the fractional-order approach to define the aforementioned description.

$$\begin{cases} {}^c_0D_t^\alpha \mathbf{X}_1(t) = -(\kappa_{(0)} + \kappa_{(1)})\mathbf{X}_1 + \kappa_{(-1)}\mathbb{H}_2\mathbf{X}_2, \\ {}^c_0D_t^\alpha \mathbf{X}_2(t) = \kappa_{(1)}\mathbf{X}_1 - \kappa_{(-1)}\mathbb{H}_2\mathbf{X}_2 + \kappa_{(-2)}\mathbf{X}_3^2 - \kappa_{(2)}\mathbf{X}_2, \\ {}^c_0D_t^\alpha \mathbf{X}_3(t) = \kappa_{(2)}\mathbf{X}_2 - \kappa_{(-2)}\mathbf{X}_3^2 - \kappa_{(3)}\mathbb{H}_2\mathbf{X}_3^2, \\ {}^c_0D_t^\alpha \mathbf{X}_4(t) = \kappa_{(3)}\mathbb{H}_2\mathbf{X}_3^2, \\ {}^c_0D_t^\alpha \mathbf{X}_5(t) = \kappa_{(0)}\mathbf{X}_1. \end{cases} \quad (1)$$

Where ${}^cD^\alpha$ represents the Caputo derivative of order $0 < \alpha \leq 1$. And

$$\mathbf{X}_1(0) \geq 0, \quad \mathbf{X}_2(0) \geq 0, \quad \mathbf{X}_3(0) \geq 0, \quad \mathbf{X}_4(0) \geq 0, \quad \mathbf{X}_5(0) \geq 0.$$

Figure (1) depicts a schematic illustration of the reaction system (1).

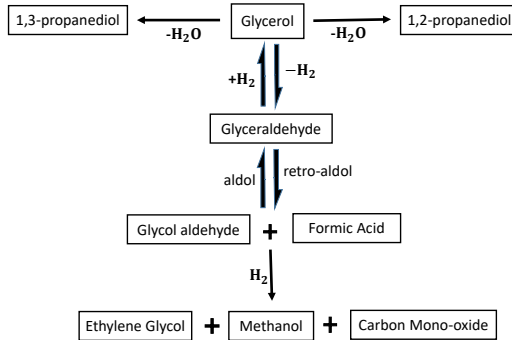


Figure 1. Glycerol conversion reaction route using Cu/ZnO catalysts

Now, let's go through a few recent and important calculus results.

Definition 1. [32] The Caputo derivative of a differentiable function $\Phi(t)$ to order $\alpha \in (0, 1)$ with beginning point, $t = 0$, is given by

$${}^c_0D_t^\alpha \Phi(t) = \frac{1}{\Gamma(1-\alpha)} \int_0^t \frac{\Phi'(q)}{(t-q)^\alpha} dq. \tag{2}$$

If $\Phi(t)$ is an integrable function with $0 < \alpha < 1$, the fractional integral is specified as follows [33]:

$${}^c_0I_t^\alpha \Phi(t) = \frac{1}{\Gamma(\alpha)} \int_0^t \frac{\Phi(q)}{(t-q)^{1-\alpha}} dq. \tag{3}$$

Lemma 1. A fixed point γ^* is regarded as the equilibrium point of the Caputo system

$${}^c_0D_t^\alpha \Phi(t) = \Phi(t, \gamma(t)), \quad \alpha \in (0, 1) \tag{4}$$

if and only if $\Phi(t, \gamma^*) = 0$.

Lemma 2. [34] Consider $\alpha \in \mathbb{R}^+$, $\eta_1(t)$, and $\eta_2(t)$ demonstrate positive functions and $\eta_3(t)$ denote an increasing as well as positive function for

$t \in [0, T]$, $T > 0$, and $\eta_3(t) \leq m$, while m is a constant value. Suppose

$$\eta_1 \leq \eta_2 + \eta_3(t) \int_0^T (t-q)^{\alpha-1} \eta_1(q) dq, \quad (5)$$

then

$$\eta_1 \leq \eta_2 E_\alpha \left[\eta_3(t) \frac{\pi \mathfrak{T}^\alpha}{\Gamma(1-\alpha) \sin(\alpha\pi)} \right]. \quad (6)$$

3 Qualitative analysis of the model

3.1 Well-posedness and positively invariant region

Theorem 1. *The solution of the proposed kinetic model (1) is distinct and limited in R_+^5 given straight-line constraints.*

Proof: We have got

$$\left\{ \begin{array}{l} \mathfrak{C}_0 D_t^\alpha \mathbf{X}_1(t) \Big|_{\mathbf{X}_1=0} = \kappa_{(-1)} \mathbb{H}_2 \mathbf{X}_2 \geq 0, \\ \mathfrak{C}_0 D_t^\alpha \mathbf{X}_2(t) \Big|_{\mathbf{X}_2=0} = \kappa_{(1)} \mathbf{X}_1 + \kappa_{(-2)} \mathbf{X}_3^2 \geq 0, \\ \mathfrak{C}_0 D_t^\alpha \mathbf{X}_3(t) \Big|_{\mathbf{X}_3=0} = \kappa_{(2)} \mathbf{X}_2 \geq 0, \\ \mathfrak{C}_0 D_t^\alpha \mathbf{X}_4(t) \Big|_{\mathbf{X}_4=0} = \kappa_{(3)} \mathbb{H}_2 \mathbf{X}_3^2 \geq 0, \\ \mathfrak{C}_0 D_t^\alpha \mathbf{X}_5(t) \Big|_{\mathbf{X}_5=0} = \kappa_{(0)} \mathbf{X}_1 \geq 0. \end{array} \right. \quad (7)$$

The choice of solution can't escape from the hyperplane if

$$\{\mathbf{X}_1(0), \mathbf{X}_2(0), \mathbf{X}_3(0), \mathbf{X}_4(0), \mathbf{X}_5(0)\} \in R_+^5.$$

The vector field on each hyperplane surrounding the non-negative orthant directs into the domain R_+^5 , making it a positively invariant set.

3.2 Equilibrium points

The nonnegative equilibria for the kinetic model specified by (1) are provided [20] by

$$(\mathbf{X}_1^*, \mathbf{X}_2^*, \mathbf{X}_3^*, \mathbf{X}_4^*, \mathbf{X}_5^*) = (0, 0, 0, \mathbf{X}_{4eq}, \mathbf{X}_{5eq}), \quad (8)$$

where $\mathbf{X}_{4eq} + \mathbf{X}_{5eq} = \mathbf{X}_1(0)$.

3.3 Solutions' existence and uniqueness

This section proves the existence and uniqueness of a solution to the system (1) by applying the Banach fixed point theory and Schaefer's fixed point theorem. Arrange the following function:

$$\begin{cases} K(t, \mathbf{X}_1, \mathbf{X}_2, \mathbf{X}_3, \mathbf{X}_4, \mathbf{X}_5) = -(\kappa_{(0)} + \kappa_{(1)})\mathbf{X}_1 + \kappa_{(-1)}\mathbb{H}_2\mathbf{X}_2, \\ L(t, \mathbf{X}_1, \mathbf{X}_2, \mathbf{X}_3, \mathbf{X}_4, \mathbf{X}_5) = \kappa_{(1)}\mathbf{X}_1 - \kappa_{(-1)}\mathbb{H}_2\mathbf{X}_2 + \kappa_{(-2)}\mathbf{X}_3^2 - \kappa_{(2)}\mathbf{X}_2, \\ M(t, \mathbf{X}_1, \mathbf{X}_2, \mathbf{X}_3, \mathbf{X}_4, \mathbf{X}_5) = \kappa_{(2)}\mathbf{X}_2 - \kappa_{(-2)}\mathbf{X}_3^2 - \kappa_{(3)}\mathbb{H}_2\mathbf{X}_3^2, \\ N(t, \mathbf{X}_1, \mathbf{X}_2, \mathbf{X}_3, \mathbf{X}_4, \mathbf{X}_5) = \kappa_{(3)}\mathbb{H}_2\mathbf{X}_3^2, \\ P(t, \mathbf{X}_1, \mathbf{X}_2, \mathbf{X}_3, \mathbf{X}_4, \mathbf{X}_5) = \kappa_{(0)}\mathbf{X}_1. \end{cases} \quad (9)$$

Therefore, the fractional integral will be applied to the initial conditions of the Caputo fractional derivative model (1) of order $\alpha > 0$. The technique results in the second type of Volterra-integral equations, which contain the solution to the proposed model (1).

$$\begin{cases} \mathbf{X}_1(t) - \mathbf{X}_1(0) = \frac{1}{\Gamma(\alpha)} \int_0^t (t-q)^{\alpha-1} K(q, \mathbf{X}_1(q)) dq, \\ \mathbf{X}_2(t) - \mathbf{X}_2(0) = \frac{1}{\Gamma(\alpha)} \int_0^t (t-q)^{\alpha-1} L(q, \mathbf{X}_2(q)) dq, \\ \mathbf{X}_3(t) - \mathbf{X}_3(0) = \frac{1}{\Gamma(\alpha)} \int_0^t (t-q)^{\alpha-1} M(q, \mathbf{X}_3(q)) dq, \\ \mathbf{X}_4(t) - \mathbf{X}_4(0) = \frac{1}{\Gamma(\alpha)} \int_0^t (t-q)^{\alpha-1} N(q, \mathbf{X}_4(q)) dq, \\ \mathbf{X}_5(t) - \mathbf{X}_5(0) = \frac{1}{\Gamma(\alpha)} \int_0^t (t-q)^{\alpha-1} P(q, \mathbf{X}_4(q)) dq. \end{cases} \quad (10)$$

In order for $(\mathbb{R}, \|\cdot\|)$ to be the Banach space and $G^1([0, T])$ to be the Banach space of all known continuous functions established in $[0, T] \rightarrow \mathbb{R}$ formed with Chebyshev norm, the function $(\mathbf{X}_1, \mathbf{X}_2, \mathbf{X}_3, \mathbf{X}_4, \mathbf{X}_5) : [0, T] \times \mathbb{R} \rightarrow \mathbb{R}$ is assumed to be continuous. Due to the polynomial vector field on the right-hand side of (9), it is \mathbb{C}^∞ and, more specifically, locally Lipschitz.

Theorem 2. *Assume that the functions $(\mathbf{X}_1, \mathbf{X}_2, \mathbf{X}_3, \mathbf{X}_4, \mathbf{X}_5) : [0, T] \times \mathbb{R} \rightarrow \mathbb{R}$ are continuous and uphold the Lipschitz condition. The system (1)*

has a distinct solution if

$$(\mathbf{X}_1, \mathbf{X}_2, \mathbf{X}_3, \mathbf{X}_4, \mathbf{X}_5) \frac{\Gamma(1-\alpha) \sin(\alpha\pi) \mathfrak{P}^\alpha}{\alpha\pi} < 1. \quad (11)$$

Proof. Establish the mapping $\mathbf{W} : G^1([0, T], \mathbb{R}) \rightarrow G^1([0, T], \mathbb{R})$, where $\mathbf{W} \in (\mathbf{X}_1, \mathbf{X}_2, \mathbf{X}_3, \mathbf{X}_4, \mathbf{X}_5) : [0, T] \times \mathbb{R} \rightarrow \mathbb{R}$.

For all $\{(\mathbf{X}_{11}, \mathbf{X}_{12}), (\mathbf{X}_{21}, \mathbf{X}_{22}), (\mathbf{X}_{31}, \mathbf{X}_{32}), (\mathbf{X}_{41}, \mathbf{X}_{42}), (\mathbf{X}_{51}, \mathbf{X}_{52})\} \in G^1([0, T], \mathbb{R})$ and $t \in [0, T]$, we find

$$\begin{aligned} & \|\mathbf{W}(\mathbf{X}_{11}(t)) - \mathbf{W}(\mathbf{X}_{12}(t))\| \\ & \leq \frac{1}{\Gamma(\alpha)} \int_0^T (t-q)^{\alpha-1} \|K(q, \mathbf{X}_{11}(q)) - K(q, \mathbf{X}_{12}(q))\| dq \\ & \leq \frac{\Pi_K}{\Gamma(\alpha)} \int_0^T (t-q)^{\alpha-1} \|\mathbf{X}_{11}(q) - \mathbf{X}_{12}(q)\| dq \\ & \leq \frac{\Pi_K \mathfrak{P}^\alpha}{\Gamma(\alpha+1)} \|\mathbf{X}_{11} - \mathbf{X}_{12}\|_{G^1}. \end{aligned} \quad (12)$$

Likewise, we discover

$$\begin{aligned} \|\mathbf{W}(\mathbf{X}_{21}(t)) - \mathbf{W}(\mathbf{X}_{22}(t))\| & \leq \frac{\Pi_L \mathfrak{P}^\alpha}{\Gamma(\alpha+1)} \|\mathbf{X}_{21} - \mathbf{X}_{22}\|_{G^1}, \\ \|\mathbf{W}(\mathbf{X}_{31}(t)) - \mathbf{W}(\mathbf{X}_{32}(t))\| & \leq \frac{\Pi_M \mathfrak{P}^\alpha}{\Gamma(\alpha+1)} \|\mathbf{X}_{31} - \mathbf{X}_{32}\|_{G^1}, \\ \|\mathbf{W}(\mathbf{X}_{41}(t)) - \mathbf{W}(\mathbf{X}_{42}(t))\| & \leq \frac{\Pi_N \mathfrak{P}^\alpha}{\Gamma(\alpha+1)} \|\mathbf{X}_{41} - \mathbf{X}_{42}\|_{G^1}, \\ \|\mathbf{W}(\mathbf{X}_{51}(t)) - \mathbf{W}(\mathbf{X}_{52}(t))\| & \leq \frac{\Pi_P \mathfrak{P}^\alpha}{\Gamma(\alpha+1)} \|\mathbf{X}_{51} - \mathbf{X}_{52}\|_{G^1}. \end{aligned} \quad (13)$$

The fact that the condition $(\mathbf{X}_1, \mathbf{X}_2, \mathbf{X}_3, \mathbf{X}_4, \mathbf{X}_5) \frac{\Gamma(1-\alpha) \sin(\alpha\pi) \mathfrak{P}^\alpha}{\alpha\pi} < 1$ is obvious from the data. Assuming that the parameter \mathbf{W} contains a fixed point in $t \in [0, T]$ as it is a contraction mapping, the idea of Banach contraction mapping is used to show this. \blacksquare

Now, utilizing Schaefer's fixed point theorem, we examine the existence of solutions for the system.

Theorem 3. *Provided that the variables $(\mathbf{X}_1, \mathbf{X}_2, \mathbf{X}_3, \mathbf{X}_4, \mathbf{X}_5) : [0, T] \times \mathbb{R} \rightarrow \mathbb{R}$ are continuous and the fact that the constants*

$$(\Pi_{K_1}, \Pi_{L_1}, \Pi_{M_1}, \Pi_{N_1}, \Pi_{P_1}) > 0$$

exist such that

$$\begin{cases} \|K(t, \mathbf{X}_1)\| \leq \Pi_{K_1}(\psi + \|\mathbf{X}_1\|), \\ \|L(t, \mathbf{X}_2)\| \leq \Pi_{L_1}(\psi + \|\mathbf{X}_2\|), \\ \|M(t, \mathbf{X}_3)\| \leq \Pi_{M_1}(\psi + \|\mathbf{X}_3\|), \\ \|N(t, \mathbf{X}_4)\| \leq \Pi_{N_1}(\psi + \|\mathbf{X}_4\|), \\ \|P(t, \mathbf{X}_5)\| \leq \Pi_{P_1}(\psi + \|\mathbf{X}_5\|), \end{cases} \tag{14}$$

where ψ is a random number between 0 and 1, then system (1) has at least one solution.

Proof. It follows that the operator \mathbf{W} is continuous from above Theorem (2). Suppose that $\{\mathbf{X}_1^{\sigma+1}\}_\infty, \{\mathbf{X}_2^{\sigma+1}\}_\infty, \{\mathbf{X}_3^{\sigma+1}\}_\infty, \{\mathbf{X}_4^{\sigma+1}\}_\infty$ and $\{\mathbf{X}_5^{\sigma+1}\}_\infty$ be sequences such that $\mathbf{X}_1^{\sigma+1} \rightarrow \mathbf{X}_1^\sigma, \mathbf{X}_2^{\sigma+1} \rightarrow \mathbf{X}_2^\sigma, \mathbf{X}_3^{\sigma+1} \rightarrow \mathbf{X}_3^\sigma, \mathbf{X}_4^{\sigma+1} \rightarrow \mathbf{X}_4^\sigma,$ and $\mathbf{X}_5^{\sigma+1} \rightarrow \mathbf{X}_5^\sigma,$ in $G^1([0, T], \mathbb{R})$. For $t \in [0, T]$, we get

$$\begin{cases} \|\mathbf{W}(\mathbf{X}_1^{\sigma+1}(t)) - \mathbf{W}(\mathbf{X}_1^\sigma(t))\| \\ \leq \frac{1}{\Gamma(\alpha)} \int_0^t (t-q)^{\alpha-1} \|K(q, \mathbf{X}_1^{\sigma+1}(q)) - K(q, \mathbf{X}_1^\sigma(q))\| dq \\ \leq \frac{\Pi_{K_1} \mathfrak{P}^\alpha}{\Gamma(\alpha+1)} \|\mathbf{X}_1^{\sigma+1} - \mathbf{X}_1^\sigma\|_{G^1}. \end{cases} \tag{15}$$

Similarly,

$$\begin{cases} \|\mathbf{W}(\mathbf{X}_2^{\sigma+1}(t)) - \mathbf{W}(\mathbf{X}_2^\sigma(t))\| \leq \frac{\Pi_{L_1} \mathfrak{P}^\alpha}{\Gamma(\alpha+1)} \|\mathbf{X}_2^{\sigma+1} - \mathbf{X}_2^\sigma\|_{G^1}, \\ \|\mathbf{W}(\mathbf{X}_3^{\sigma+1}(t)) - \mathbf{W}(\mathbf{X}_3^\sigma(t))\| \leq \frac{\Pi_{M_1} \mathfrak{P}^\alpha}{\Gamma(\alpha+1)} \|\mathbf{X}_3^{\sigma+1} - \mathbf{X}_3^\sigma\|_{G^1}, \\ \|\mathbf{W}(\mathbf{X}_4^{\sigma+1}(t)) - \mathbf{W}(\mathbf{X}_4^\sigma(t))\| \leq \frac{\Pi_{N_1} \mathfrak{P}^\alpha}{\Gamma(\alpha+1)} \|\mathbf{X}_4^{\sigma+1} - \mathbf{X}_4^\sigma\|_{G^1}, \\ \|\mathbf{W}(\mathbf{X}_5^{\sigma+1}(t)) - \mathbf{W}(\mathbf{X}_5^\sigma(t))\| \leq \frac{\Pi_{P_1} \mathfrak{P}^\alpha}{\Gamma(\alpha+1)} \|\mathbf{X}_5^{\sigma+1} - \mathbf{X}_5^\sigma\|_{G^1}. \end{cases} \tag{16}$$

Where $\|\mathbf{X}_1^{\sigma+1} - \mathbf{X}_1^\sigma\| \rightarrow 0, \|\mathbf{X}_2^{\sigma+1} - \mathbf{X}_2^\sigma\| \rightarrow 0, \|\mathbf{X}_3^{\sigma+1} - \mathbf{X}_3^\sigma\| \rightarrow 0, \|\mathbf{X}_4^{\sigma+1} - \mathbf{X}_4^\sigma\| \rightarrow 0,$ and $\|\mathbf{X}_5^{\sigma+1} - \mathbf{X}_5^\sigma\| \rightarrow 0,$ as $\sigma \rightarrow 0$. Therefore, the operator \mathbf{W} is continuous.

On the set of $G^1([0, T], \mathbb{R})$, we then show that the operator \mathbf{W} is a one-to-one bounded function. For each $\mathbf{X}_1 \in \mathbf{B}_{\mathbf{X}_1}$, $\mathbf{X}_2 \in \mathbf{B}_{\mathbf{X}_2}$, $\mathbf{X}_3 \in \mathbf{B}_{\mathbf{X}_3}$, $\mathbf{X}_4 \in \mathbf{B}_{\mathbf{X}_4}$, $\mathbf{X}_5 \in \mathbf{B}_{\mathbf{X}_5}$, and for $\xi > 0$, there exist a constant $\varphi > 0$ such that $\{\|\mathbf{W}_{\mathbf{X}_1}\|, \|\mathbf{W}_{\mathbf{X}_2}\|, \|\mathbf{W}_{\mathbf{X}_3}\|, \|\mathbf{W}_{\mathbf{X}_4}\|, \|\mathbf{W}_{\mathbf{X}_5}\|\} \leq \varphi$. Also all the continuous functions on the range $t \in [0, T]$ are defined as a subset of Banach space by

$$\begin{cases} \mathbf{B}_{\mathbf{X}_1} = \{\mathbf{X}_1 \in G^1([0, T], \mathbb{R}) : \|\mathbf{X}_1\| \leq \xi\}, \\ \mathbf{B}_{\mathbf{X}_2} = \{\mathbf{X}_2 \in G^1([0, T], \mathbb{R}) : \|\mathbf{X}_2\| \leq \xi\}, \\ \mathbf{B}_{\mathbf{X}_3} = \{\mathbf{X}_3 \in G^1([0, T], \mathbb{R}) : \|\mathbf{X}_3\| \leq \xi\}, \\ \mathbf{B}_{\mathbf{X}_4} = \{\mathbf{X}_4 \in G^1([0, T], \mathbb{R}) : \|\mathbf{X}_4\| \leq \xi\}, \\ \mathbf{B}_{\mathbf{X}_5} = \{\mathbf{X}_5 \in G^1([0, T], \mathbb{R}) : \|\mathbf{X}_5\| \leq \xi\}. \end{cases} \quad (17)$$

Hence, for any $t \in [0, T]$,

$$\begin{aligned} \|\mathbf{W}\mathbf{X}_1\| &\leq \|\mathbf{X}_1(0)\| + \frac{1}{\Gamma(\alpha)} \int_0^t (t-q)^{\alpha-1} \|\mathbf{K}(q, \mathbf{X}_1(q))\| dq \\ &\leq \|\mathbf{X}_1(0)\| + \frac{\|\mathbf{K}(q, \mathbf{X}_1(q))\|}{\Gamma(\alpha)} \int_0^t (t-q)^{\alpha-1} dq \\ &\leq \|\mathbf{X}_1(0)\| + \Pi_{\mathbf{K}_1}(\psi + \|\mathbf{X}_1\|) \left[\frac{\mathfrak{P}^\alpha}{\Gamma(\alpha+1)} \right] \\ &\leq \|\mathbf{X}_1(0)\| + \Pi_{\mathbf{K}_1}(\psi + \xi) \left[\frac{\mathfrak{P}^\alpha}{\Gamma(\alpha+1)} \right]. \end{aligned} \quad (18)$$

And

$$\begin{aligned} \|\mathbf{W}\mathbf{X}_2\| &\leq \|\mathbf{X}_2(0)\| + \Pi_{L_1}(\psi + \xi) \left[\frac{\mathfrak{P}^\alpha}{\Gamma(\alpha+1)} \right], \\ \|\mathbf{W}\mathbf{X}_3\| &\leq \|\mathbf{X}_3(0)\| + \Pi_{M_1}(\psi + \xi) \left[\frac{\mathfrak{P}^\alpha}{\Gamma(\alpha+1)} \right], \\ \|\mathbf{W}\mathbf{X}_4\| &\leq \|\mathbf{X}_4(0)\| + \Pi_{N_1}(\psi + \xi) \left[\frac{\mathfrak{P}^\alpha}{\Gamma(\alpha+1)} \right], \\ \|\mathbf{W}\mathbf{X}_5\| &\leq \|\mathbf{X}_5(0)\| + \Pi_{P_1}(\psi + \xi) \left[\frac{\mathfrak{P}^\alpha}{\Gamma(\alpha+1)} \right]. \end{aligned} \quad (19)$$

Consider the opposite scenario when \mathbf{W} maps bounded sets in $G^1([0, T], \mathbb{R})$ into equal continuous sets. If $0 \leq t_i \leq t_j \leq T$, $\{t_i, t_j\} \in [0, T]$, and $\mathbf{X}_1 \in \mathbf{B}_{\mathbf{X}_1}$, $\mathbf{X}_2 \in \mathbf{B}_{\mathbf{X}_2}$, $\mathbf{X}_3 \in \mathbf{B}_{\mathbf{X}_3}$, $\mathbf{X}_4 \in \mathbf{B}_{\mathbf{X}_4}$, $\mathbf{X}_5 \in \mathbf{B}_{\mathbf{X}_5}$ then

$$\left\{ \begin{aligned} & \|\mathbf{W}\mathbf{X}_1(t_i) - \mathbf{W}\mathbf{X}_1(t_j)\| \\ & \leq \frac{1}{\Gamma(\alpha)} \left\| \int_0^{t_i} [(t_i - q)^{\alpha-1} - (t_j - q)^{\alpha-1}] \mathbf{K}(q, \mathbf{X}_1(q)) dq \right\| \\ & \quad + \frac{1}{\Gamma(\alpha)} \left\| \int_{t_i}^{t_j} (t_j - q)^{\alpha-1} \mathbf{K}(q, \mathbf{X}_1(q)) dq \right\| \\ & \leq \frac{\Pi_{\mathbf{K}_1}(\psi + \xi)}{\Gamma(\alpha)} \left\| \int_0^{t_i} [(t_i - q)^{\alpha-1} - (t_j - q)^{\alpha-1}] dq + \int_{t_i}^{t_j} (t_j - q)^{\alpha-1} dq \right\| \\ & \leq \frac{\Pi_{\mathbf{K}_1}(\psi + \xi) \mathfrak{P}^\alpha}{\Gamma(\alpha+1)} [t_i^\alpha - t_j^\alpha + 2(t_j - t_i)^\alpha]. \end{aligned} \right. \quad (20)$$

And

$$\left\{ \begin{aligned} & \|\mathbf{W}\mathbf{X}_2(t_i) - \mathbf{W}\mathbf{X}_2(t_j)\| \leq \frac{\Pi_{\mathbf{L}_1}(\psi + \xi) \mathfrak{P}^\alpha}{\Gamma(\alpha+1)} [t_i^\alpha - t_j^\alpha + 2(t_j - t_i)^\alpha], \\ & \|\mathbf{W}\mathbf{X}_3(t_i) - \mathbf{W}\mathbf{X}_3(t_j)\| \leq \frac{\Pi_{\mathbf{M}_1}(\psi + \xi) \mathfrak{P}^\alpha}{\Gamma(\alpha+1)} [t_i^\alpha - t_j^\alpha + 2(t_j - t_i)^\alpha], \\ & \|\mathbf{W}\mathbf{X}_4(t_i) - \mathbf{W}\mathbf{X}_4(t_j)\| \leq \frac{\Pi_{\mathbf{N}_1}(\psi + \xi) \mathfrak{P}^\alpha}{\Gamma(\alpha+1)} [t_i^\alpha - t_j^\alpha + 2(t_j - t_i)^\alpha], \\ & \|\mathbf{W}\mathbf{X}_5(t_i) - \mathbf{W}\mathbf{X}_5(t_j)\| \leq \frac{\Pi_{\mathbf{P}_1}(\psi + \xi) \mathfrak{P}^\alpha}{\Gamma(\alpha+1)} [t_i^\alpha - t_j^\alpha + 2(t_j - t_i)^\alpha]. \end{aligned} \right. \quad (21)$$

The aforementioned expressions tend to zero when $t_i \rightarrow t_j$ on the right side of the inequality. \mathbf{W} is a continuous function in accordance with the Arzela-Ascoli theorem. Now we demonstrate that

$$\begin{aligned} \mathbf{Z}(\mathbf{W}) &= \{(\mathbf{X}_1, \mathbf{X}_2, \mathbf{X}_3, \mathbf{X}_4, \mathbf{X}_5) \in G^1([0, T], \mathbb{R}) : (\mathbf{X}_1, \mathbf{X}_2, \mathbf{X}_3, \mathbf{X}_4, \mathbf{X}_5) \\ &= \varphi(\mathbf{X}_1, \mathbf{X}_2, \mathbf{X}_3, \mathbf{X}_4, \mathbf{X}_5)\} \end{aligned} \quad (22)$$

is bounded for some $0 < \varphi < 1$ by (1). For every $t \in [0, T]$, let $(\mathbf{X}_1, \mathbf{X}_2, \mathbf{X}_3, \mathbf{X}_4, \mathbf{X}_5) \in \mathbf{Z}(\mathbf{W})$, such that $(\mathbf{X}_1, \mathbf{X}_2, \mathbf{X}_3, \mathbf{X}_4, \mathbf{X}_5) = \varphi \mathbf{W}(\mathbf{X}_1, \mathbf{X}_2, \mathbf{X}_3, \mathbf{X}_4, \mathbf{X}_5)$, yields

$$\left\{ \begin{aligned} & \|\mathbf{X}_1(t)\| \leq \mathbf{X}_1(0) + \frac{1}{\Gamma(\alpha)} \int_0^T (t - q)^{\alpha-1} \|\mathbf{K}(q, \mathbf{X}_1(q))\| dq \\ & \leq \mathbf{X}_1(0) + \frac{\Pi_{\mathbf{K}_1}}{\Gamma(\alpha)} \int_0^T (t - q)^{\alpha-1} (\psi + \|\mathbf{X}_1(q)\|) dq \\ & \leq \mathbf{X}_1(0) + \frac{\psi \Pi_{\mathbf{K}_1}}{\Gamma(\alpha)} \int_0^T (t - q)^{\alpha-1} dq + \frac{\Pi_{\mathbf{K}_1}}{\Gamma(\alpha)} \int_0^T (t - q)^{\alpha-1} \|\mathbf{X}_1(q)\| dq \\ & \leq \mathbf{X}_1(0) + \frac{\Pi_{\mathbf{K}_1} \mathfrak{P}^\alpha}{\Gamma(\alpha+1)} + \frac{\Pi_{\mathbf{K}_1} \mathfrak{P}^\alpha}{\Gamma(\alpha+1)} \int_0^T (t - q)^{\alpha-1} \|\mathbf{X}_1(q)\| dq \\ & \leq \left\{ \mathbf{X}_1(0) + \frac{\Pi_{\mathbf{K}_1} \mathfrak{P}^\alpha}{\Gamma(\alpha+1)} \mathbf{K}_\alpha(\Pi_{\mathbf{K}_1} \mathfrak{P}^\alpha) \right\} < \infty \end{aligned} \right. \quad (23)$$

And

$$\begin{aligned}
 \|\mathbf{X}_2(t)\| &\leq \left\{ \mathbf{X}_2(0) + \frac{\Pi_{L_1} \mathfrak{P}^\alpha}{\Gamma(\alpha + 1)} L_\alpha(\Pi_{L_1} \mathfrak{P}^\alpha) \right\} < \infty, \\
 \|\mathbf{X}_3(t)\| &\leq \left\{ \mathbf{X}_3(0) + \frac{\Pi_{M_1} \mathfrak{P}^\alpha}{\Gamma(\alpha + 1)} M_\alpha(\Pi_{M_1} \mathfrak{P}^\alpha) \right\} < \infty, \\
 \|\mathbf{X}_4(t)\| &\leq \left\{ \mathbf{X}_4(0) + \frac{\Pi_{N_1} \mathfrak{P}^\alpha}{\Gamma(\alpha + 1)} N_\alpha(\Pi_{N_1} \mathfrak{P}^\alpha) \right\} < \infty, \\
 \|\mathbf{X}_5(t)\| &\leq \left\{ \mathbf{X}_5(0) + \frac{\Pi_{P_1} \mathfrak{P}^\alpha}{\Gamma(\alpha + 1)} P_\alpha(\Pi_{N_1} \mathfrak{P}^\alpha) \right\} < \infty.
 \end{aligned} \tag{24}$$

The system (1)'s solution exists because \mathbf{W} has a fixed point, which is shown by Schaefer's fixed point theorem, as $\mathbf{Z}(\mathbf{W})$ is limited. \blacksquare

3.4 Generalized Ulam-Hyers-Rassias (UHR) stability

We evaluate the stability of the system (1) to demonstrate that it is UHR stable using the Ulam-Hyers-Rassias (UHR) stability technique as given in [34].

Definition 2. The proposed system (1) is generalized Ulam-Hyers-Rassias (UHR) stable with respect to $\mu(t) \in G^1([0, T], \mathbb{R})$ if there exists real values $\{\lambda_\gamma, \lambda_\tau, \lambda_\vartheta, \lambda_\rho, \lambda_\nu\} > 0$ with $\{\gamma, \tau, \vartheta, \rho, \nu\} > 0$ and for all solutions $(\mathbf{X}_1, \mathbf{X}_2, \mathbf{X}_3, \mathbf{X}_4, \mathbf{X}_5) \in G^1([0, T], \mathbb{R})$ of the subsequent inequalities

$$\begin{aligned}
 |{}^c D_t^\alpha \mathbf{X}_1(t) - K(t, \mathbf{X}_1(t))| &\leq \mu(t), \\
 |{}^c D_t^\alpha \mathbf{X}_2(t) - L(t, \mathbf{X}_2(t))| &\leq \mu(t), \\
 |{}^c D_t^\alpha \mathbf{X}_3(t) - M(t, \mathbf{X}_3(t))| &\leq \mu(t), \\
 |{}^c D_t^\alpha \mathbf{X}_4(t) - N(t, \mathbf{X}_4(t))| &\leq \mu(t), \\
 |{}^c D_t^\alpha \mathbf{X}_5(t) - P(t, \mathbf{X}_5(t))| &\leq \mu(t),
 \end{aligned} \tag{25}$$

there exists a solution $(\bar{\mathbf{X}}_1, \bar{\mathbf{X}}_2, \bar{\mathbf{X}}_3, \bar{\mathbf{X}}_4, \bar{\mathbf{X}}_5) \in G^1([0, T], \mathbb{R})$ of proposed

system (1) with

$$\begin{cases} |\mathbf{X}_1(t) - \bar{\mathbf{X}}_1(t)| \leq \lambda_\gamma \mu(t), \\ |\mathbf{X}_2(t) - \bar{\mathbf{X}}_2(t)| \leq \lambda_\tau \mu(t), \\ |\mathbf{X}_3(t) - \bar{\mathbf{X}}_3(t)| \leq \lambda_\vartheta \mu(t), \\ |\mathbf{X}_4(t) - \bar{\mathbf{X}}_4(t)| \leq \lambda_\rho \mu(t), \\ |\mathbf{X}_5(t) - \bar{\mathbf{X}}_5(t)| \leq \lambda_\nu \mu(t). \end{cases} \tag{26}$$

Theorem 4. *The proposed system (1) is generalized Ulam-Hyers-Rassias stable with regard to $G^1([0, T], \mathbb{R})$ if*

$$(\mathbf{X}_1, \mathbf{X}_2, \mathbf{X}_3, \mathbf{X}_4, \mathbf{X}_5)\mathfrak{P}^\alpha < 1. \tag{27}$$

Proof. There exists $\mathfrak{S} = \{\gamma, \tau, \vartheta, \rho, \nu\} > 0$ such that

$$\int_0^t (t - q)\mu(q) dq \leq \mathfrak{S}\mu(t) \tag{28}$$

is true for all $t \in [0, T]$ in relation to definition (2), which assigns μ as a non-decreasing function of t . The continuous nature of the functions $\mathbf{X}_1, \mathbf{X}_2, \mathbf{X}_3, \mathbf{X}_4,$ and \mathbf{X}_5 has been proved, and the Lipschitz condition is met when $(\mathbf{X}_1, \mathbf{X}_2, \mathbf{X}_3, \mathbf{X}_4, \mathbf{X}_5) > 0$. Theorem (2) provides a unique solution for the proposed system (1)

$$\begin{cases} \bar{\mathbf{X}}_1(t) = \mathbf{X}_1(0) + \frac{1}{\Gamma(\alpha)} \int_0^t (t - q)^{\alpha-1} \|K(q, \bar{\mathbf{X}}_1(q))\| dq, \\ \bar{\mathbf{X}}_2(t) = \mathbf{X}_2(0) + \frac{1}{\Gamma(\alpha)} \int_0^t (t - q)^{\alpha-1} \|L(q, \bar{\mathbf{X}}_2(q))\| dq, \\ \bar{\mathbf{X}}_3(t) = \mathbf{X}_3(0) + \frac{1}{\Gamma(\alpha)} \int_0^t (t - q)^{\alpha-1} \|M(q, \bar{\mathbf{X}}_3(q))\| dq, \\ \bar{\mathbf{X}}_4(t) = \mathbf{X}_4(0) + \frac{1}{\Gamma(\alpha)} \int_0^t (t - q)^{\alpha-1} \|N(q, \bar{\mathbf{X}}_4(q))\| dq, \\ \bar{\mathbf{X}}_5(t) = \mathbf{X}_5(0) + \frac{1}{\Gamma(\alpha)} \int_0^t (t - q)^{\alpha-1} \|P(q, \bar{\mathbf{X}}_5(q))\| dq. \end{cases} \tag{29}$$

When we integrate the inequalities in the definition (2), we acquire

$$\begin{aligned} & \left| \mathbf{X}_1(t) - \mathbf{X}_1(0) - \frac{1}{\Gamma(\alpha)} \int_0^t (t - q)^{\alpha-1} K(q, \mathbf{X}_1(q)) dq \right| \\ & \leq \frac{1}{\Gamma(\alpha)} \int_0^t (t - q)^{\alpha-1} \mu(q) dq \leq \frac{\gamma\mu(t)\mathfrak{P}^\alpha}{\Gamma(\alpha + 1)}. \end{aligned} \tag{30}$$

From equation (30) and Lemma (2), we have

$$\left\{ \begin{aligned} & |\mathbf{X}_1(t) - \bar{\mathbf{X}}_1(t)| \\ & \leq |\mathbf{X}_1(t) - \mathbf{X}_1(0) - [\frac{1}{\Gamma(\alpha)} \int_0^t (t-q)^{\alpha-1} \mathbf{K}(q, \bar{\mathbf{X}}_1(q)) dq \\ & \quad + \frac{1}{\Gamma(\alpha)} \int_0^t (t-q)^{\alpha-1} \mathbf{K}(q, \mathbf{X}_1(q)) dq - \frac{1}{\Gamma(\alpha)} \int_0^t (t-q)^{\alpha-1} \mathbf{K}(q, \mathbf{X}_1(q)) dq]| \\ & \leq |\mathbf{X}_1(t) - \mathbf{X}_1(0) - \frac{1}{\Gamma(\alpha)} \int_0^t (t-q)^{\alpha-1} \mathbf{K}(q, \mathbf{X}_1(q)) dq| \\ & \quad + \frac{1}{\Gamma(\alpha)} \int_0^t (t-q)^{\alpha-1} |\mathbf{K}(q, \mathbf{X}_1(q)) - \mathbf{K}(q, \bar{\mathbf{X}}_1(q))| dq \\ & \leq \frac{\gamma \mu(t) \mathfrak{P}^\alpha}{\Gamma(\alpha+1)} + \frac{\Pi_{\mathbf{K}} \mathfrak{P}^\alpha}{\Gamma(\alpha+1)} \int_0^t (t-q)^{\alpha-1} |\mathbf{X}_1(q) - \bar{\mathbf{X}}_1(q)| dq \\ & \leq \frac{\gamma \mu(t) \mathfrak{P}^\alpha}{\Gamma(\alpha+1)} \mathbb{E}_\alpha(\Pi_{\mathbf{K}} \mathfrak{P}^\alpha). \end{aligned} \right. \quad (31)$$

Let $\frac{\gamma \mu(t) \mathfrak{P}^\alpha}{\Gamma(\alpha+1)} \mathbf{K}_\alpha(\Pi_{\mathbf{K}} \mathfrak{P}^\alpha) = \varpi_\gamma$, then we have

$$|\mathbf{X}_1(t) - \bar{\mathbf{X}}_1(t)| \leq \varpi_\gamma \mu(t). \quad (32)$$

■

4 Numerical scheme

It has been suggested in the literature that the power-law kernel-based Caputo derivative is ideal for simulating power-law processes in real-world issues. We numerically solve the system (1) using a Newton polynomial-based approach. To make the system (1) simpler to use, we will write it as follows:

$$\begin{aligned} Z_1(t, \mathbf{X}_1) &= -(\kappa_{(0)} + \kappa_{(1)}) \mathbf{X}_1 + \kappa_{(-1)} \mathbb{H}_2 \mathbf{X}_2, \\ Z_2(t, \mathbf{X}_2) &= \kappa_{(1)} \mathbf{X}_1 - \kappa_{(-1)} \mathbb{H}_2 \mathbf{X}_2 + \kappa_{(-2)} \mathbf{X}_3^2 - \kappa_{(2)} \mathbf{X}_2, \\ Z_3(t, \mathbf{X}_3) &= \kappa_{(2)} \mathbf{X}_2 - \kappa_{(-2)} \mathbf{X}_3^2 - \kappa_{(3)} \mathbb{H}_2 \mathbf{X}_3^2, \\ Z_4(t, \mathbf{X}_4) &= \kappa_{(3)} \mathbb{H}_2 \mathbf{X}_3^2, \\ Z_5(t, \mathbf{X}_5) &= \kappa_{(0)} \mathbf{X}_1. \end{aligned} \quad (33)$$

Following the use of fractional integral, we arrive at:

$$\begin{aligned}
 \mathbf{X}_1(t_j + 1) &= \mathbf{X}_1(0) + \frac{1}{\Gamma(\alpha)} \sum_{u=2}^j \int_{t_u}^{t_{u+1}} Z_1(t, \mathbf{X}_1)(t_{j+1} - q)^{\alpha-1} dq, \\
 \mathbf{X}_2(t_j + 1) &= \mathbf{X}_2(0) + \frac{1}{\Gamma(\alpha)} \sum_{u=2}^j \int_{t_u}^{t_{u+1}} Z_2(t, \mathbf{X}_2)(t_{j+1} - q)^{\alpha-1} dq, \\
 \mathbf{X}_3(t_j + 1) &= \mathbf{X}_3(0) + \frac{1}{\Gamma(\alpha)} \sum_{u=2}^j \int_{t_u}^{t_{u+1}} Z_3(t, \mathbf{X}_3)(t_{j+1} - q)^{\alpha-1} dq, \quad (34) \\
 \mathbf{X}_4(t_j + 1) &= \mathbf{X}_4(0) + \frac{1}{\Gamma(\alpha)} \sum_{u=2}^j \int_{t_u}^{t_{u+1}} Z_4(t, \mathbf{X}_4)(t_{j+1} - q)^{\alpha-1} dq, \\
 \mathbf{X}_5(t_j + 1) &= \mathbf{X}_5(0) + \frac{1}{\Gamma(\alpha)} \sum_{u=2}^j \int_{t_u}^{t_{u+1}} Z_4(t, \mathbf{X}_5)(t_{j+1} - q)^{\alpha-1} dq.
 \end{aligned}$$

Now let's examine the Newton polynomial:

$$\begin{aligned}
 \mathbf{P}(t, \mathbf{X}) &\simeq \mathbf{P}(t_{j-2}, \mathbf{X}^{j-2}) + \frac{1}{\delta t} \left\{ \mathbf{P}(t_{j-1}, \mathbf{X}^{j-1}) - \mathbf{P}(t_{j-2}, \mathbf{X}^{j-2}) \right\} \\
 &\times (q - t_{j-2}) + \frac{1}{2\delta t^2} \left\{ \mathbf{P}(t_j, \mathbf{X}^j) - 2\mathbf{P}(t_{j-2}, \mathbf{X}^{j-1}) \right. \\
 &\left. + \mathbf{P}(t_{j-2}, \mathbf{X}^{j-2}) \right\} \times (q - t_{j-2})(q - t_{j-1}) \quad (35)
 \end{aligned}$$

Replacing the Newton polynomial (35) into equation (34), we find

$$\left\{ \begin{aligned}
 &\mathbf{X}_1^{(j+1)} \\
 &= \mathbf{X}_1(0) + \frac{1}{\Gamma(\alpha)} \sum_{u=2}^j Z_1(t_{u-2}, \mathbf{X}_1^{u-2}) \times \int_{t_u}^{t_{u+1}} (t_{j+1} - q)^{\alpha-1} dq \\
 &+ \frac{1}{\Gamma(\alpha)} \sum_{u=2}^j \frac{1}{\delta t} \left[Z_1(t_{u-1}, \mathbf{X}_1^{u-1}) - Z_1(t_{u-2}, \mathbf{X}_1^{u-2}) \right] \\
 &\times \int_{t_u}^{t_{u+1}} (q - t_{u-2})(t_{j+1} - q)^{\alpha-1} dq \\
 &+ \frac{1}{\Gamma(\alpha)} \sum_{u=2}^j \frac{1}{2\delta t^2} \left[Z_1(t_u, \mathbf{X}_1^u) - 2Z_1(t_{u-1}, \mathbf{X}_1^{u-1}) \right. \\
 &\left. + Z_1(t_{u-2}, \mathbf{X}_1^{u-2}) \right] \times \int_{t_u}^{t_{u+1}} (q - t_{u-2})(q - t_{u-1})(t_{j+1} - q)^{\alpha-1} dq
 \end{aligned} \right. \quad (36)$$

Putting the values of the integral shown in the aforementioned equation, we achieve

$$\left\{ \begin{aligned} \mathbf{X}_1(t_{j+1}) &= \mathbf{X}_1(0) + \frac{(\delta t)^\alpha}{\Gamma(\alpha+1)} \sum_{u=2}^j Z_1(t_{u-2}, \mathbf{X}_1^{u-2}) \times Y_1 \\ &+ \frac{(\delta t)^\alpha}{\Gamma(\alpha+2)} \sum_{u=2}^j \left[Z_1(t_{u-1}, \mathbf{X}_1^{u-1}) - Z_1(t_{u-2}, \mathbf{X}_1^{u-2}) \right] \times Y_2 \\ &+ \frac{\alpha(\delta t)^\alpha}{2\Gamma(\alpha+3)} \sum_{u=2}^j \left[Z_1(t_u, \mathbf{X}_1^u) - 2Z_1(t_{u-1}, \mathbf{X}_1^{u-1}) \right. \\ &\left. + Z_1(t_{u-2}, \mathbf{X}_1^{u-2}) \right] \times Y_3. \end{aligned} \right. \quad (37)$$

Where,

$$\left\{ \begin{aligned} Y_1 &= (j-u+1)^\alpha - (j-u)^\alpha \\ Y_2 &= (j-u+1)^\alpha(j-u+3+2\alpha) - (j-u)^\alpha(j-u+3+3\alpha) \\ Y_3 &= (j-u+1)^\alpha \left[2(j-u)^2 + (3\alpha+10)(j-u) + 2\alpha^2 + 9\alpha + 12 \right] \\ &\quad - (j-u)^\alpha \left[2(j-u)^2 + (5\alpha+10)(j-u) + 6\alpha^2 + 18\alpha + 12 \right]. \end{aligned} \right.$$

Likewise, we find

$$\left\{ \begin{aligned} \mathbf{X}_2(t_{j+1}) &= \mathbf{X}_2(0) + \frac{(\delta t)^\alpha}{\Gamma(\alpha+1)} \sum_{u=2}^j Z_2(t_{u-2}, \mathbf{X}_2^{u-2}) \times Y_1 \\ &+ \frac{(\delta t)^\alpha}{\Gamma(\alpha+2)} \sum_{u=2}^j \left[Z_2(t_{u-1}, \mathbf{X}_2^{u-1}) - Z_2(t_{u-2}, \mathbf{X}_2^{u-2}) \right] \times Y_2 \\ &+ \frac{\alpha(\delta t)^\alpha}{2\Gamma(\alpha+3)} \sum_{u=2}^j \left[Z_2(t_u, \mathbf{X}_2^u) - 2Z_2(t_{u-1}, \mathbf{X}_2^{u-1}) \right. \\ &\left. + Z_2(t_{u-2}, \mathbf{X}_2^{u-2}) \right] \times Y_3. \end{aligned} \right. \quad (38)$$

$$\left\{ \begin{aligned} \mathbf{X}_3(t_{j+1}) &= \mathbf{X}_3(0) + \frac{(\delta t)^\alpha}{\Gamma(\alpha+1)} \sum_{u=2}^j Z_3(t_{u-2}, \mathbf{X}_3^{u-2}) \times Y_1 \\ &+ \frac{(\delta t)^\alpha}{\Gamma(\alpha+2)} \sum_{u=2}^j \left[Z_3(t_{u-1}, \mathbf{X}_3^{u-1}) - Z_3(t_{u-2}, \mathbf{X}_3^{u-2}) \right] \times Y_2 \\ &+ \frac{\alpha(\delta t)^\alpha}{2\Gamma(\alpha+3)} \sum_{u=2}^j \left[Z_3(t_u, \mathbf{X}_3^u) - 2Z_3(t_{u-1}, \mathbf{X}_3^{u-1}) \right. \\ &\left. + Z_3(t_{u-2}, \mathbf{X}_3^{u-2}) \right] \times Y_3. \end{aligned} \right. \quad (39)$$

$$\left\{ \begin{aligned} \mathbf{X}_4(t_{j+1}) &= \mathbf{X}_4(0) + \frac{(\delta t)^\alpha}{\Gamma(\alpha+1)} \sum_{u=2}^j Z_4(t_{u-2}, \mathbf{X}_4^{u-2}) \times Y_1 \\ &+ \frac{(\delta t)^\alpha}{\Gamma(\alpha+2)} \sum_{u=2}^j \left[Z_4(t_{u-1}, \mathbf{X}_4^{u-1}) - Z_4(t_{u-2}, \mathbf{X}_4^{u-2}) \right] \times Y_2 \\ &+ \frac{\alpha(\delta t)^\alpha}{2\Gamma(\alpha+3)} \sum_{u=2}^j \left[Z_4(t_u, \mathbf{X}_4^u) - 2Z_4(t_{u-1}, \mathbf{X}_4^{u-1}) \right. \\ &\left. + Z_4(t_{u-2}, \mathbf{X}_4^{u-2}) \right] \times Y_3. \end{aligned} \right. \quad (40)$$

$$\left\{ \begin{aligned} \mathbf{X}_5(t_{j+1}) &= \mathbf{X}_5(0) + \frac{(\delta t)^\alpha}{\Gamma(\alpha+1)} \sum_{u=2}^j Z_5(t_{u-2}, \mathbf{X}_5^{u-2}) \times Y_1 \\ &+ \frac{(\delta t)^\alpha}{\Gamma(\alpha+2)} \sum_{u=2}^j \left[Z_5(t_{u-1}, \mathbf{X}_5^{u-1}) - Z_5(t_{u-2}, \mathbf{X}_5^{u-2}) \right] \times Y_2 \\ &+ \frac{\alpha(\delta t)^\alpha}{2\Gamma(\alpha+3)} \sum_{u=2}^j \left[Z_5(t_u, \mathbf{X}_5^u) - 2Z_5(t_{u-1}, \mathbf{X}_5^{u-1}) \right. \\ &\left. + Z_5(t_{u-2}, \mathbf{X}_5^{u-2}) \right] \times Y_3. \end{aligned} \right. \quad (41)$$

5 Numerical simulation

The model's numerical simulations have been carried out using the generalized two-step Lagrange polynomial for the power law kernel and the parametric values from [20]. The simulations of the suggested systems are shown in figures (2)-(21). For these simulations, we employed several fractional order values $\alpha = 1.0, 0.95, 0.90, 0.85$. Figures (2)-(6) show simulations of the advised model for equal initial amounts of glycerol and hydrogen at different fractional orders under the Caputo operator. We utilized initial concentrations as $\mathbf{X}_1 = 1, \mathbf{X}_2 = \mathbf{X}_3 = \mathbf{X}_4 = \mathbf{X}_5 = 0$. When we start with hydrogen:glycerol(H:G) ratio of 1:1, Figures (2)-(6) show that the glycerol (\mathbf{X}_1) is quickly transformed into the products at higher fractional orders. As the fractional order increases, so does the synthesis of glyceraldehyde (\mathbf{X}_2) and glycolaldehyde (\mathbf{X}_3). At high fractional orders, more ethylene glycol (\mathbf{X}_4) will be produced than propanediol (\mathbf{X}_5). Figures (7)-(11) show simulations of the suggested model for a 2:1 proportion of hydrogen to glycerol. In figures (7)-(11), we utilized initial concentrations as $\mathbf{X}_1 = 2, \mathbf{X}_2 = \mathbf{X}_3 = \mathbf{X}_4 = \mathbf{X}_5 = 0$. At larger fractional orders, increasing the amount of hydrogen over that of glycerol still boosts the creation of ethylene glycol over propanediol, according to the figures (7)-(11).

Figures (12)-(16) show the findings obtained when the hydrogen to glycerol ratio was set at 1:1 as well as $\kappa_0, \kappa_2, \kappa_{-2}, \kappa_3$, and simply modifying κ_1 and κ_{-1} . When the hydrogen used is twice as much as the original glycerol, the model simulations obtained are illustrated in Figures (17)-(21), along with the modified parameter values used for the simulation. Figures (12)-(21) demonstrate that raising the values of κ_1 and κ_{-1} increases the concentra-

tion of ethylene glycol (\mathbf{X}_4) generated and causes the reaction to approach equilibrium faster. This is because, as shown in system (1), an increase in these constants causes higher glycolaldehyde (\mathbf{X}_3) to be made, which causes higher glyceraldehyde (\mathbf{X}_2) to be generated, resulting in an increment in the ethylene glycol (\mathbf{X}_4) produced. Glycerol breaks down quickly with greater fractional orders, and the generation of products increases. Fractional order derivations are more effective at comprehending chemical processes than classical order, and the recommended model provides useful feedback for non-integer fractional parameter values.

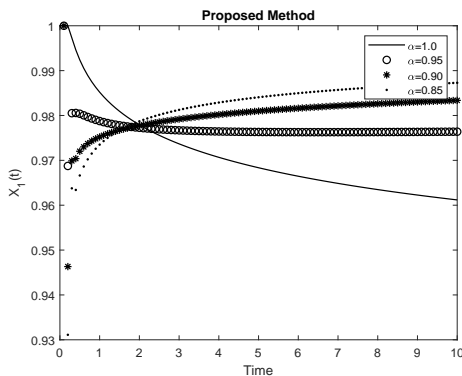


Figure 2. Simulation of Glycerol (\mathbf{X}_1) at H:G ratio of 1:1.

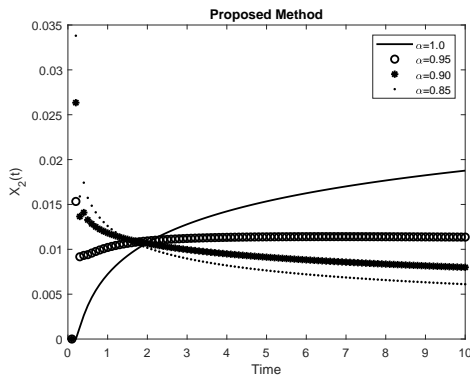


Figure 3. Simulation of Glyceraldehyde (\mathbf{X}_2) at H:G ratio of 1:1.

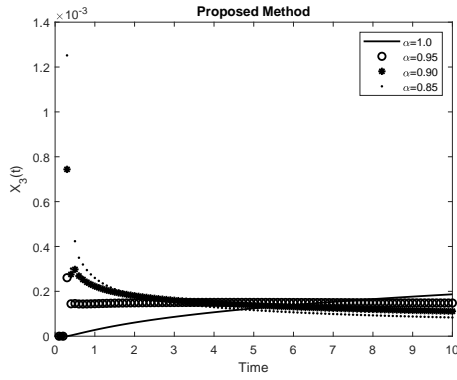


Figure 4. Simulation of Glycolaldehyde (X_3) at H:G ratio of 1:1.

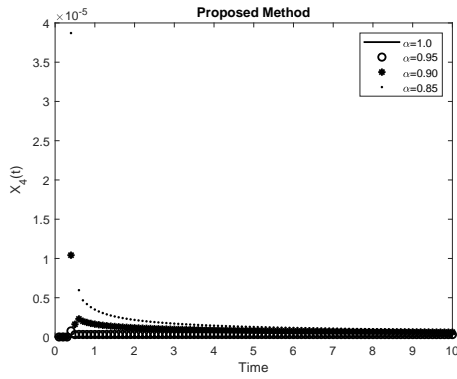


Figure 5. Simulation of Ethylene Glycol (X_4) at H:G ratio of 1:1.

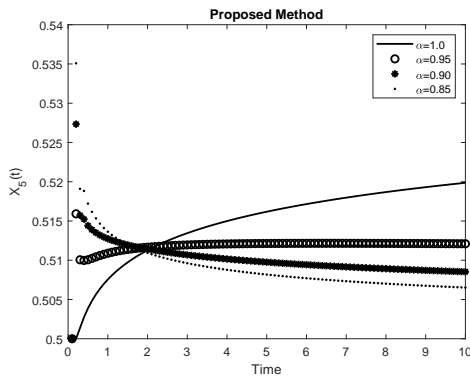


Figure 6. Simulation of Propanediol (X_5) at H:G ratio of 1:1.

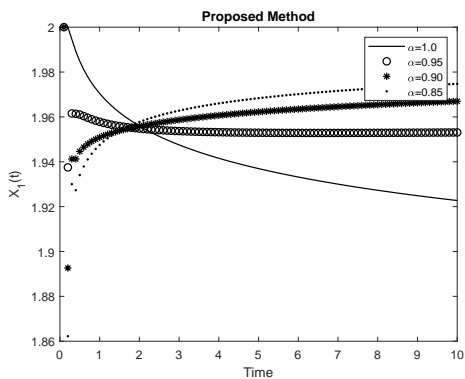


Figure 7. Simulation of Glycerol (X_1) at H:G ratio of 2:1.

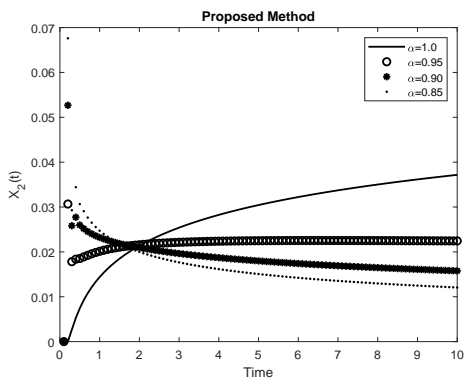


Figure 8. Simulation of Glyceraldehyde (X_2) at H:G ratio of 2:1.

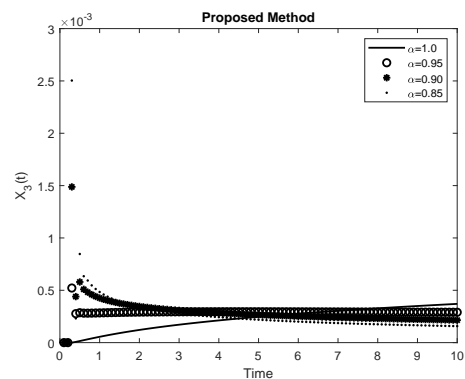


Figure 9. Simulation of Glycolaldehyde (X_3) at H:G ratio of 2:1.

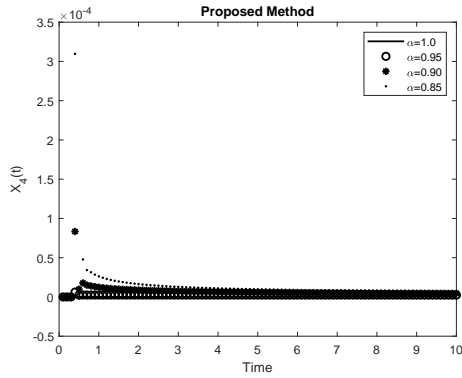


Figure 10. Simulation of Ethylene Glycol (X_4) at H:G ratio of 2:1.

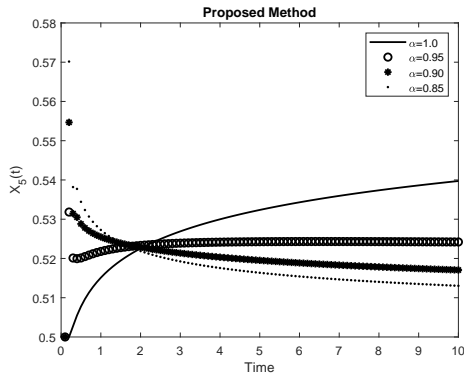


Figure 11. Simulation of Propanediol (X_5) at H:G ratio of 2:1.

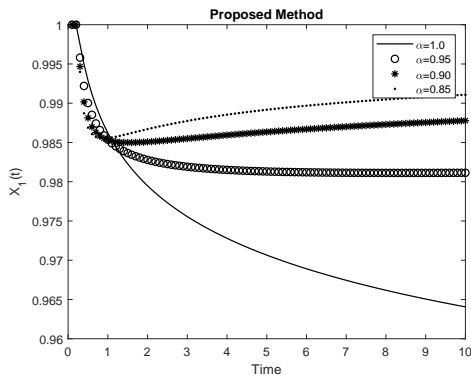


Figure 12. Simulation of Glycerol (X_1) at H:G ratio of 1:1.

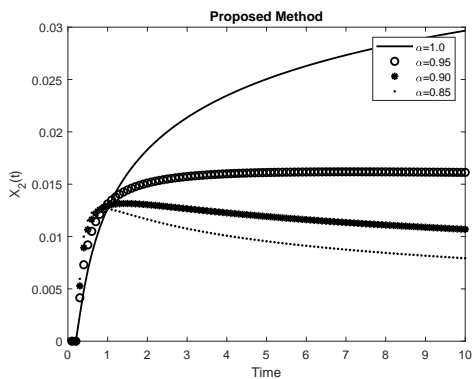


Figure 13. Simulation of Glyceraldehyde (X_2) at H:G ratio of 1:1.

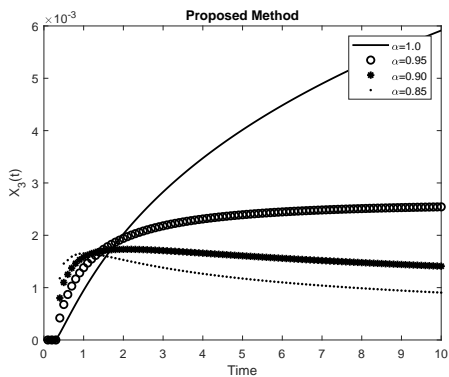


Figure 14. Simulation of Glycolaldehyde (X_3) at H:G ratio of 1:1.

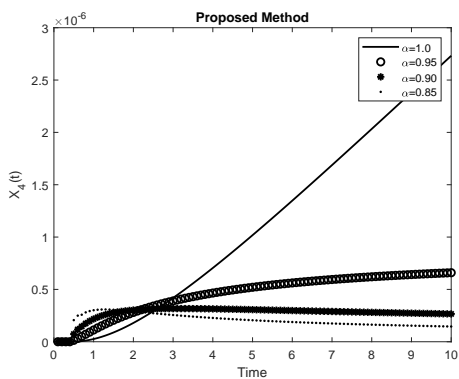


Figure 15. Simulation of Ethylene Glycol (X_4) at H:G ratio of 1:1.

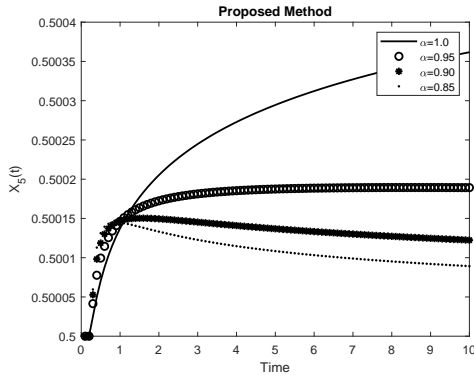


Figure 16. Simulation of Propanediol (X_5) at H:G ratio of 1:1.

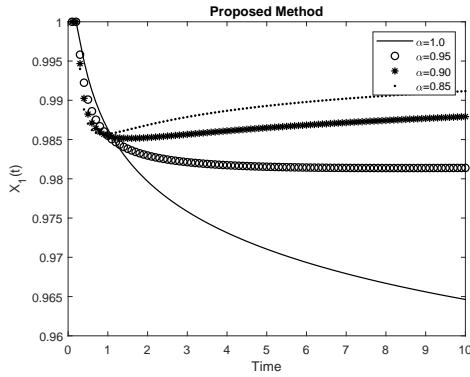


Figure 17. Simulation of Glycerol (X_1) at H:G ratio of 2:1.

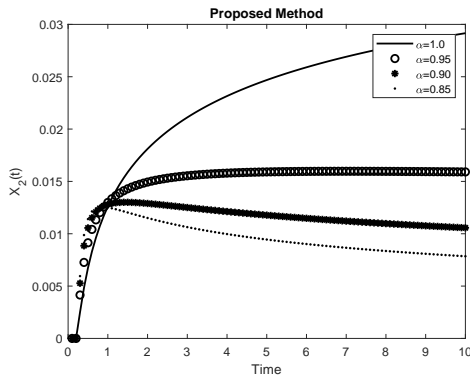


Figure 18. Simulation of Glyceraldehyde (X_2) at H:G ratio of 2:1.

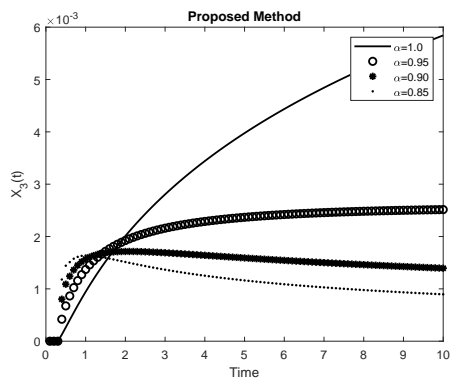


Figure 19. Simulation of Glycolaldehyde (X_3) at H:G ratio of 2:1.

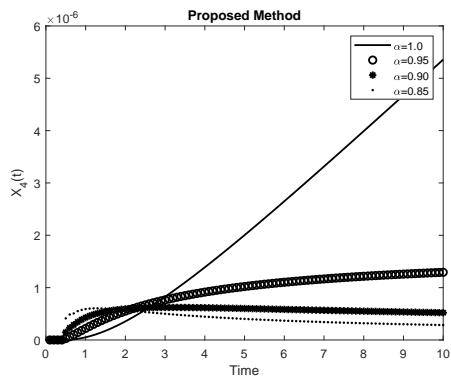


Figure 20. Simulation of Ethylene Glycol (X_4) at H:G ratio of 2:1.

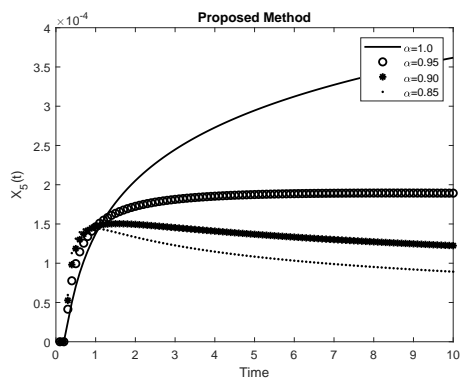


Figure 21. Simulation of Propanediol (X_5) at H:G ratio of 2:1.

6 Conclusion

In this study, we created a fractional order kinetic model to investigate the hydrogenolysis of glycerol, and the simulations of the model were consistent with the chemistry of the reaction. The model has positive, constrained solutions, as demonstrated by our investigation of the positively invariant region. We also used techniques from a number of fixed point theorems to investigate the existence and uniqueness of the model. Our findings demonstrate the generalized Ulam-Hyers-Rassias stability of the model. A numerical approach based on Newton's polynomial interpolation was subsequently used to resolve the mathematical model. There are noticeable differences between the results using various fractional numbers. The flexibility and behavior of the solution curves are significantly impacted by non-integer order, as is seen on graphs. All model solutions depend on the chosen hydrogen to glycerol ratio and reaction constant values, but they all converge to a stable limit point in a two-dimensional plane of a positive cone in the R^5 space. The ability to replicate memory effects is the main advantage of the fractional order kinetic model. When compared to classical model, fractional model have a higher degree of freedom, making it ideal for best fitting real data when it is available. This significant complex catalytic process can be better understood by using the tools of the suggested approach. It is possible to broaden this research to include more generally applicable fractional operators and enhance the control methods for turning glycerol into useable end products.

Acknowledgment: This work is supported by National Natural Science Foundation of China (No.12261015, No.62062018), Project of High-level Innovative Talents of Guizhou Province ([2016]5651), Guizhou Key Laboratory of Big Data Statistical Analysis(No.[2019]5103), University Science and Technology Top Talents Project of Guizhou Province (KY[2018]047)

References

- [1] M. Williamson, B. A. Ball, Soil biogeochemical responses to multiple co-occurring forms of human-induced environmental change, *Oecologia* (2023) **201** 1109–1121.
- [2] M. A. U. Waqih, N. A. Bhutto, N. H. Ghumro, S. Kumar, M. A. Salam, Rising environmental degradation and impact of foreign direct investment: an empirical evidence from SAARC region, *J. Environ. Manag.* **243** (2019) 472–480.
- [3] D. Lüthi, M. Le Floch, B. Bereiter, T. Blunier, J. M. Barnola, U. Siegenthaler, D. Raynaud, High-resolution carbon dioxide concentration record 650,000–800,000 years before present, *Nature* **453** (2008) 379–382.
- [4] A. M. Driga, A. S. Drigas, Climate change 101: How everyday activities contribute to the ever-growing issue, *Int. J. Recent Contributions Eng. Sci. IT* **7**(2009) 22–31.
- [5] S. J. Malode, K. K. Prabhu, R. J. Mascarenhas, N. P. Shetti, T. M. Aminabhavi, Recent advances and viability in biofuel production, *Energy Convers. Manag.* **10X** (2021) #100070.
- [6] H. Taher, S. Al-Zuhair, The use of alternative solvents in enzymatic biodiesel production: a review, *Biofuel Bioprod. Biorefin.* **11** (2017) 168–194.
- [7] P. Verma, M. P. Sharma, Review of process parameters for biodiesel production from different feedstocks, *Renew. sustain. energy rev.* **62** (2016) 1063–1071.
- [8] F. G. Calvo-Flores, M. J. Monteagudo-Arrebola, J. A. Dobado, J. Isac-García, Green and bio-based solvents, *Top. Curr. Chem.* **376** (2018) 1–40.
- [9] A. A. Abdul Raman, H. W. Tan, A. Buthiyappan, Two-step purification of glycerol as a value added by product from the biodiesel production process, *Front. Chem.* **7** (2019) #774.
- [10] H. Zhao, L. Zheng, X. Li, P. Chen, Z. Hou, Hydrogenolysis of glycerol to 1, 2-propanediol over Cu-based catalysts: A short review, *Catal. Today* **355** (2020) 84–95.
- [11] J. J. Bozell, G. R. Petersen, Technology development for the production of biobased products from biorefinery carbohydrates—the US

- Department of Energy's "Top 10" revisited, *Green Chem.* **12** (2010) 539–554.
- [12] C. Wang, H. Jiang, C. Chen, R. Chen, W. Xing, Solvent effect on hydrogenolysis of glycerol to 1, 2-propanediol over Cu-ZnO catalyst, *Chem. Eng. J.* **264** (2015) 344–350.
- [13] M. R. Nanda, Z. Yuan, W. Qin, C. J. Xu, Recent advancements in catalytic conversion of glycerol into propylene glycol: A review, *Catal. Rev.* **58**(2016) 309-336.
- [14] M. L. Shoji, V. D. B. C. Dasireddy, S. Singh, A. Govender, P. Mohlala, H. B. Friedrich, The effect of rhenium on the conversion of glycerol to mono-alcohols over nickel catalysts under continuous flow conditions, *Sustain. Energy Fuels.* **3** (2019) 2038–2047.
- [15] M. J. Gilkey, B. Xu, Heterogeneous catalytic transfer hydrogenation as an effective pathway in biomass upgrading, *ACS Catal.* **6** (2016) 1420–1436.
- [16] M. L. Shoji, V. D. B. C. Dasireddy, S. Singh, P. Mohlala, D. J. Morgan, S. Iqbal, H. B. Friedrich, An investigation of Cu-Re-ZnO catalysts for the hydrogenolysis of glycerol under continuous flow conditions, *Sustain. Energy Fuels.* **1** (2017) 1437–1445.
- [17] Z. Xi, W. Jia, Z. Zhu, $\text{WO}_3\text{-ZrO}_2\text{-TiO}_2$ composite oxide supported pt as an efficient catalyst for continuous hydrogenolysis of glycerol, *Catal. Lett.* **151** (2021) 124-137.
- [18] N. N. Pandhare, S. M. Pudi, S. Mondal, K. Pareta, M. Kumar, P. Biswas, Development of kinetic model for hydrogenolysis of glycerol over Cu/MgO catalyst in a slurry reactor, *Ind. Eng. Chem. Res.* **57** (2018) 101–110.
- [19] S. Mondal, H. Malviya, P. Biswas, Kinetic modelling for the hydrogenolysis of bio-glycerol in the presence of a highly selective Cu–Ni– Al_2O_3 catalyst in a slurry reactor, *React. Chem. Eng.* **4** (2019) 595–609.
- [20] F. P. Costa, T. Q. Ndlovu, M. Shoji, Mathematical investigations of a kinetic model for glycerol hydrogenolysis via heterogeneous catalysis, *MATCH Commun. Math. Comput. Chem.* **88** (2022) 437–460.
- [21] M. Farman, A. Shehzad, A. Akgül, D. Baleanu, M. D. Sen, Modelling and analysis of a measles epidemic model with the constant proportional Caputo operator, *Symmetry* **15** (2023) #468.

-
- [22] C. J. Xu, Z. X. Liu, Y. C. Pang, S. Saifullah, M. Inc, Oscillatory, crossover behavior and chaos analysis of HIV-1 infection model using piece-wise Atangana-Baleanu fractional operator: Real data approach, *Chaos Solit. Fract.* **164** (2022) #112662.
- [23] M. U. Akram, N. Abbas, M. Farman, S. Manzoor, M. I. Khan, S. M. Osman, R. Luque, A. Shanableh, Tumor micro-environment sensitive release of doxorubicin through chitosan based polymeric nanoparticles: An in-vitro study, *Chemosphere* **313** (2023) #137332.
- [24] M. Aslam, M. Farman, H. Ahmad, T. N. Gia, A. Ahmad, S. Askar, Fractal fractional derivative on chemistry kinetics hires problem, *AIMS Math.* **7** (2022) 1155–1184.
- [25] K. M. Saad, Comparing the Caputo, Caputo-Fabrizio and Atangana-Baleanu derivative with fractional order: Fractional cubic isothermal auto-catalytic chemical system, *Eur. Phys. J. Plus.* **133** (2018) 1–12.
- [26] C. J. Xu, D. Mu, Z. X. Liu, Y. C. Pang, M. X. Liao, P. L. Li, Bifurcation dynamics and control mechanism of a fractional-order delayed Brusselator chemical reaction model, *MATCH Commun. Math. Comput. Chem.* **89** (2023) 73–106.
- [27] M. Khan, Z. Ahmad, F. Ali, N. Khan, I. Khan, K.S. Nisar, Dynamics of two-step reversible enzymatic reaction under fractional derivative with Mittag-Leffler Kernel, *PLoS One* **18** (2023) #e0277806.
- [28] S. Chen, T. Chen, J. Chu, C. J. Xu, Global stabilization of uncertain nonlinear systems via fractional-order PID, *Commun. Nonlin. Sci. Num. Simul.* **116** (2023) #106838.
- [29] P. Li, Y. Lu, C. J. Xu, J. Ren, Insight into Hopf bifurcation and control methods in fractional order BAM neural networks incorporating symmetric structure and delay, *Cogn. Comput.* (2023) 1–43.
- [30] K. S. Nisar, M. Farman, E. Hincal, A. Shehzad, Modelling and analysis of bad impact of smoking in society with constant proportional-Caputo Fabrizio operator, *Chaos Solit. Fract.* **172** (2023) # 113549.
- [31] P. Li, R. Gao, C. J. Xu, Y. Li, A. Akgül, D. Baleanu, Dynamics exploration for a fractional-order delayed zooplankton-phytoplankton system, *Chaos Solit. Fract.* **166** (2023) #112975.
- [32] M. Caputo, Linear models of dissipation whose Q is almost frequency independent-II, *Geophys J. Int.* **13** (1967) 529–539.

- [33] M. Farman, C. Alfiniyah, A. Shehzad, Modelling and analysis tuberculosis (TB) model with hybrid fractional operator, *Alex. Eng. J.* **72** (2023) 463–478.
- [34] U. B. Odionyenma, N. Ikenna, B. Bolaji, Analysis of a model to control the co-dynamics of chlamydia and gonorrhoea using Caputo fractional derivative, *Math. Model. Numer. Anal. Appl.* **2** (2023) 111–140.